Optics final project: Optical interference with digital holograms

Garrido-Islas, Donaldo A011275416@itesm.mx
Sánchez-Bernal, Sebastián. A01339431@itesm.mx
Vega-Lezama, Rodrigo. A01329614@itesm.mx
Tecnológico de Monterrey, Campus Monterrey, Departamento de Física

1 Abstract

This text its a theoretical and numerical approach of a paper from the American Journal of Physics [1]. It uses the principles proposed by Thomas Young in his famous double-slit experiment in order to analyze the different fringe patterns that occur due to light interference and demonstrate that these fringes happen not only in the intensity of the resulting pattern but also in other properties, such as polarization and orbital angular momentum. We show how we can digitally create and study interference setups based on a variety of apertures and pinhole arrangements. Then we explain conceptually the effects of the changes on the apertures on the resulting fringes, and provide code and information to recreate the experiments using a MATLAB environment.

2 Introduction

Before the origins of modern physics, light was understood as a particle that inhabited the so-called Ether. Later on, in history, the scientific community held a constant debate on whether light was actually a particle (as stated in the corpuscular theory of light) or a wave (as defended by physicists such as Christiaan Huygens and Robert Hooke), since different data and experimental results provided evidence to support both claims. It was not until the beginnings of the 19th century, that an English scientist named Thomas Young made a controversial yet revolutionary proposal, in which he used Newton's work and his famous double-slit experiment to prove that light could interfere with itself, similar to the way water waves did. This was a change of paradigm in the notion that scientists of that time had about light, and thanks to Young's discovery and calculations, mankind is nowadays able to produce technology such as radio astronomy, 3D-imaging, and the Laser Interferometer Gravitational-Wave Observatory (LIGO).

Although Young's conclusions are almost always referred to interference fringes in intensity (bright and dark stripes), our purpose is to explore and discuss two more characteristics of light that present fringes as well: orbital angular momentum and polarization. In this work, we approach the interference phenomenon through two sets of conjugate variables of light: linear position and linear momentum, and angular position and angular momentum, and we review the mathematical and physical differences between the Fourier analysis of these two sets. Moreover, we provide information on how to reproduce and interpret the results numerically. The text is organized in the following manner: Section 3.1 revisits the principles for fringes in intensity and gives an introductory approach to wave interference. Section 3.2 presents the bases of the Spatial Light Modulator and offers a series of plots to aid the reader understand its holographic use. Section 3.3 studies fringes in polarization, and section 3.4 proposes an inspection of fringes in OAM through the study of angular position and momentum.

3 Main results and Discussion

3.1 Fringes in intensity

Interference in intensity is often classified into two types: constructive and destructive. A mathematical representation of interference for two monochromatic waves of light on the same plane can be obtained through the following analysis:

$$E_1 = Ae^{i(\omega t - \varphi_1)} \tag{1}$$

and

$$E_2 = Ae^{i(\omega t - \varphi_2)} \tag{2}$$

where A represents the amplitude of both waves, and φ_1 and φ_2 are the respective phases of each field. We can then represent the superposition of both waves as:

$$E = E_1 + E_2 = Ae^{i\omega t}e^{-i(\varphi_1+\varphi_2)} \tag{3}$$

Computing the square module of E, we obtain the intensity of the interaction between both waves:

$$I = |E|^2 = 4A^2 \cos^2\left(\frac{\varphi_1 - \varphi_2}{2}\right) \tag{4}$$

From this result, it is easy to observe that whenever the difference in phases is a multiple of $2n\pi$, the intensity will be at its maximum possible amplitude, resulting thus in a constructive interference (for n being any integer, including zero). On the other hand, if the different in phases is a multiple of $(2n-1)\pi$, the expression will be zero, representing then a destructive interference.

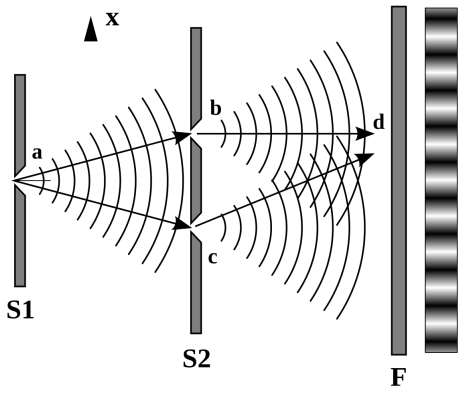

Figure 1: Visual representation of Young's experiment. Constructive interference occurs in those points on the screen where both waves are completely in phase. Destructive interference occurs in those points on the screen where both waves have a phase difference of π. A phase difference other than that will give some kind of interference, not completely constructive nor destructive.

An important note on this result for the intensity of the fringes is that it does not rely on any specific coordinate system, since the values of φ_1 and φ_2 are independent of the geometry. We can therefore have light beams whose phase depends on the azimuthal angle, on the form of $exp(-il\theta)$, where l is the topological charge. This concept will be relevant when we analyze fringes in orbital angular momentum, at the last part of this section.

3.2 Digitally creating fringes

In the multiple experiments performed for the creation of this paper, the principal optical object was the Spatial Light Modulator (SLM). This device allows the user to modulate the phase and intensity of an incident beam, letting you store holographic data in order to create different optical arrangements. These objects use a liquid crystal display that control the birefringence.

To reproduce the multiple apertures of the paper, we used MATLAB (Codes in Appendix B). The bases for this reproduction were the geometrical symmetries that the apertures presents to shape them, and then, putting a blazed grating. We placed the grating to separate the undiffracted zeroth-order and the diffracted first-order light that passes through the SLM, since the SLM allows us only to encode information on the polarization component parallel to the liquid crystal molecules. The digital pinholes are shown in figure 2a, they were created to be superposed with a blazed grating (figure 12b) that changes its phase in a diagonal form. The fringes in azimutal direction were simulated by the develop of the image of the superposition of two OAM modes (figure 2c) and then, located over the blazed grating as observed in figure 2d. The radial fringes were obtained creating a ring of the form of a ring (figure 2e) and once again, we simulate removing the undiffracted component from the diffracted component, putting a grating over the hologram, as we see in figure 2f.

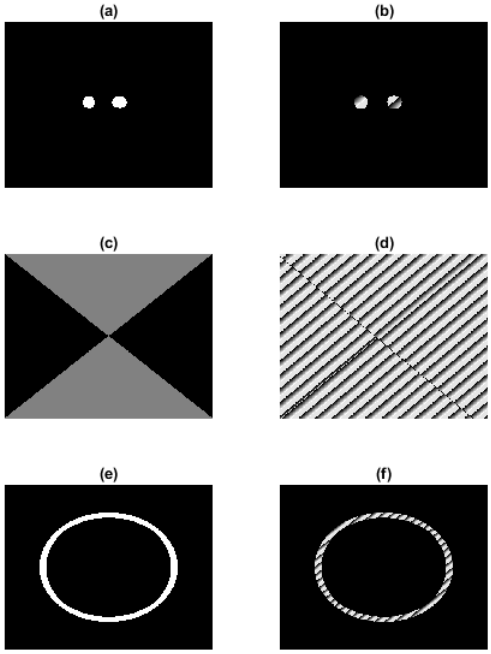

Figure 2: Simulation of the fringes created by the SLM. In the left side, the fringes. In the right side, the pattern after collocating the blazed grating over the .

To model the experimental fringes (linear, azimuthal and radial) displayed in the paper, we use a numerical approach (codes in Appendix B subsection 5.2.2). The results of this code are shown in the next figures. In the first three plots (Figure 3) it is possible to observe how a bigger distance between

the apertures increases the number of interference fringes. The figure 4 shows the different patterns generated by the superposition of different Laguerre-Gauss modes with $l = 1, 2, 3$. In order to model the modes, we use the following mathematical expression in our code to describe the Laguerre-Gauss beams:

$$f_{m,n}(\mathbf{r}) = \left[\frac{\sqrt{2}r_\perp}{w(z)}\right]^m \mathrm{L}_m^n\left(\frac{2r_\perp^2}{w^2(z)}\right) \cdot e^{in\phi} e^{i(2m+n)\varphi(z)} e^{-\frac{r^2}{w^2(z)}} \quad (5)$$

The last plot (Figure 5) shows the interference pattern of a multiple circular aperture arrange. To calculate the patterns, we use the Fraunhofer diffraction integral in our code.

$$U(\mathbf{r}) = \frac{1}{i\lambda_0 z} e^{ik_0 z} e^{\frac{ik_0}{2z}\left(x^2+y^2\right)} \cdot \iint_{-\infty}^{\infty} U\left(x_0, y_0, 0\right) e^{-\frac{ik_0}{z}(x_0 x + y_0 y)} dx_0 dy_0 \quad (6)$$

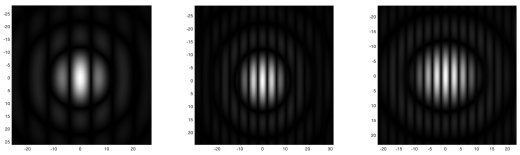

Figure 3: Young experiment with variation in the distance between the apertures.

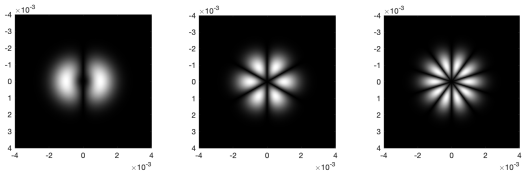

Figure 4: Superposition of OAM modes |l|=1,3,5

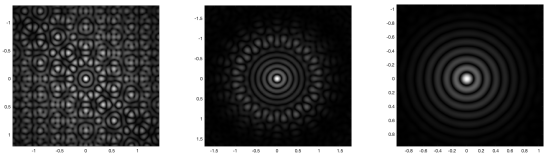

Figure 5: Interference pattern for the arrange of small circular apertures

In addition to the experimental part performed in the paper, we decided to develop a numerical approach to an arrange of circular apertures in spiral form, to have a better understanding of these phenomena and study its behavior in scenarios different to the ones proposed by the original paper. We show the results in the figure 6.

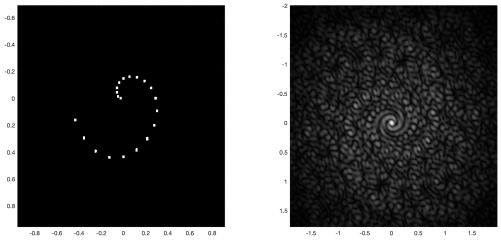

Figure 6: Interference of a spiral arrange with circular apertures.

3.3 Fringes in polarization

Let's consider the addition of two electromagnetic waves that have orthogonal polarization. It is not possible to see interference in the intensity pattern of this fields, but in this case we also analyze the polarization of the resultant field, where the interference fringes can be seen. Using MATLAB, we generated the diagonal and antidiagonal projections, the resulting intensity pattern of adding the projections and the polarization maps.

The polarization is defined in terms of the time variation of the electric field direction $\mathbf{E}(\mathbf{r}, t)$ in the point $\mathbf{r}$. We can write this vector field as:

$$\mathbf{E} = E_{0x}\cos\left(kz - \omega t + \varphi_1\right)\hat{\mathbf{x}} + E_{0y}\cos\left(kz - \omega t + \varphi_2\right)\hat{\mathbf{y}} \quad (7)$$

Where z is the direction of propagation, φ_1 and φ_2 are the phases asociated with the vertical and horizontal components, $k = 2\pi/\lambda$, t is the time and ω is angular frequency. With this definition, we can write the equation for the polarization ellipse that represents the general polarization state:

$$\left(\frac{E_x}{E_{0x}}\right)^2 + \left(\frac{E_y}{E_{0y}}\right)^2 - 2\frac{E_x}{E_{0x}}\frac{E_y}{E_{0y}}\cos\delta = \sin^2\delta \quad (8)$$

where $\delta = \varphi_1 - \varphi_2$. We used the determination of the electric field on each coordinate system to create the maps of polarization that we see in figures 7, 8 and 9. For the linear case we used the definition $\varphi_1 = k_1 x, \varphi_2 = k_2 x$, for the radial polarization we used $\varphi_1 = k_\rho \rho, \varphi_2 = 0, \rho = \sqrt{x^2 + y^2}$ and for the azimutal $\varphi_1 = l\theta, \varphi_2 = -l\theta, \theta = \tan^{-1}(y/x)$. After we obtained the different Electric field components, we could use the definition of the vector stokes:

$$S_0 = |E_x|^2 + |E_y|^2$$

$$S_1 = |E_x|^2 - |E_y|^2$$

$$S_2 = 2Re(E_x \bar{E_y})$$

$$S_3 = 2\mathcal{I}m(E_x \bar{E_y})$$

and the parameter $L = S_1 + iS_2$ and $I_p = \sqrt{S_1^2 + S_2^2 + S_3^2}$ to obtain the major semi-axis A,

the minor semi-axis B, the inclination angle α and the helicity H:

$$A = \sqrt{\frac{1}{2}(I_p + |L|)}, \quad \alpha = \frac{1}{2}\arg(L)$$

$$B = \sqrt{\frac{1}{2}(I_p - |L|)}, \quad H = sign(S3)$$

Once we had these four parameters, we were able to make the parametrical plots.
To create the figures that are shown below, we used the codes that are in the appendix D. To obtain the diagonal projection in figure 7 we made a computational model of Young double slit experiment using the equation 6 and to get the antidiagonal component we put a half-wave plate in one aperture like the researchers experimentally do in the original paper. For the figure 8 we used the next Bessel beam expression and add an extra term of $n\pi/l$ to move the rings.

$$E(r_0, z) = J_n(ar_0) \cdot \exp(in\theta_0) \exp\left[-\frac{(r_0 - b)^2}{w_0^2}\right] \quad (9)$$

For the figure 9 we use the Laguerre-Gauss expression (Equation 5) to represent a beam with OAM modes. The diagonal and antidiagonal are the same beams with a $\pi/2$ rotation. The intensity pattern is obtained when you add the two projections.

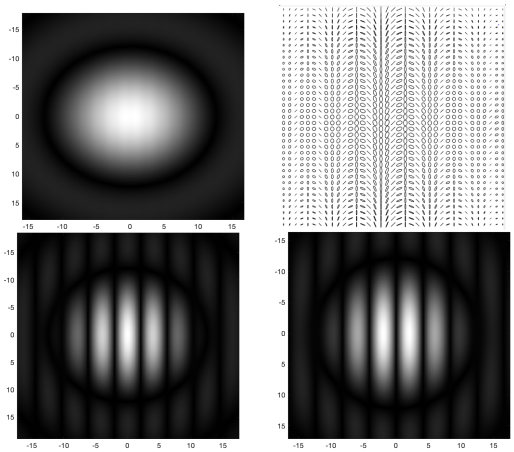

Figure 7: Intensity pattern, polarization map, diagonal projection and antidiagonal projection

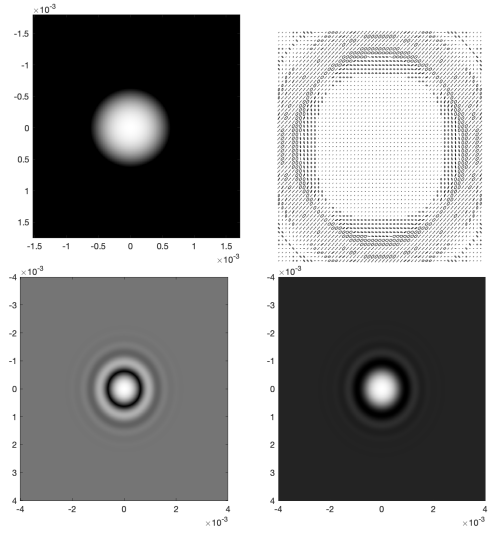

Figure 8: Intensity pattern, polarization map, diagonal projection and antidiagonal projection

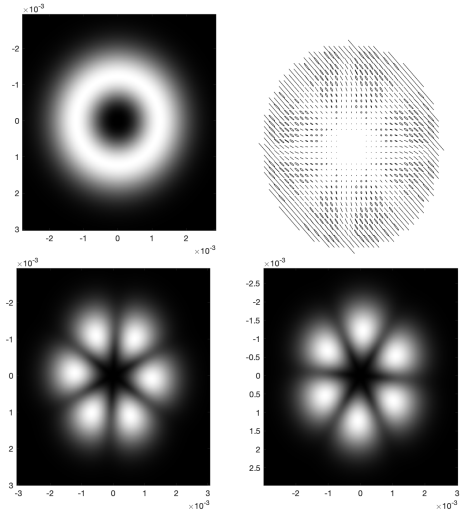

Figure 9: Intensity pattern, polarization map, diagonal projection and antidiagonal projection

3.4 Fringes in orbital angular momentum

As mentioned earlier in the introductory section, the purpose of this work is to present as well the notion of fringes in orbital angular momentum (OAM). We will do so by analyzing how Heisenberg's uncertainty principle, which ultimately leads to the interference phenomenon, applies not only to *linear* position and momentum but also *angular* position and momentum. Experimentally, $\Delta\phi$ errors are due to the non-linearity of the spatial light modulator, and Δl errors are due to noise in the detection system. As shown in Fig. 10, for small angular uncertainties, $\Delta\phi\Delta l = \hbar/2$.

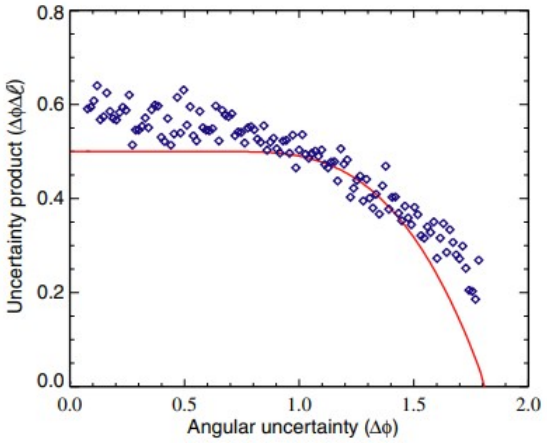

Figure 10: Experimental (diamonds) and theoretical (line) relationship between the product of the uncertainties in angular position and angular momentum in units of $\hbar$ plotted against the uncertainty in angular position

It is relevant to review how position and momentum are related through the Fourier transform, which is a mathematical representation of the far-field propagation in optical physics. One of the principal differences between working in an angular reference frame rather than a linear one, is that due to the periodicity of the angular position, its relationship with OAM is through a discrete Fourier transform, rather than a continuous one:

$$\tilde{\psi}_l = \frac{1}{\sqrt{2\pi}} \int \psi(\theta) \exp(-il\theta) d\theta \tag{10}$$

and

$$\psi(\theta) = \frac{1}{\sqrt{2\pi}} \sum_{-\infty}^{\infty} \tilde{\psi}_l \exp(il\theta) \tag{11}$$

where $\theta \in [0, 2\pi]$. Instead of having, then, slits with mere x or y components, we are now able to work with slits that open for a specific angle, in a cake slice-like shape (a restriction of the angular range within an optical beam profile generates OAM sidebands on the transmitted light, which visually produces these angular diffraction patterns). This allows us to represent the field $\psi(\theta)$ in terms of the angular location and the size of the "slice" (which we will call ϵ), resulting in the following expression for intensity:

$$I_l = \frac{2\epsilon^2}{\pi} sinc^2(\epsilon l/2) \cos^2(\pi l/2) \tag{12}$$

The mathematical development for these results can be found in Appendix E. Note that since Eq. 12 is valid for discrete values of l, as previously mentioned, the expression only survive to even values of l, due to the cosine term.

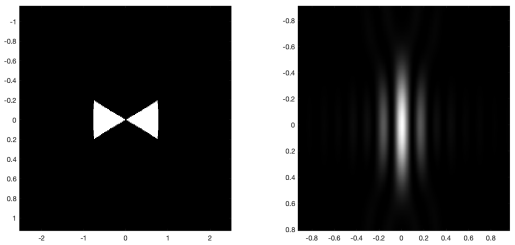

Figure 11: Interference of azimutal apertures.

Figure 11 presents a visual numerical interpretation of the interference pattern (right) from the cake-like slices (left). It is clear how, unlike linear interference, azimutal interference is enveloped by the squared sinc term in the expression of its intensity. If we were able to look experimentally at the OAM content of the diffracted beam, we would notice the fringe behavior only for discrete OAM value.

4 Conclusion

In conclusion, the general approach of the original paper was to analyze interference fringes of light beams in many observables. Therefore, the principal purpose of our project was to recreate the experimental results in a theoretical and numerical way. We found that the computational results (i.e. interference and polarization patterns) are really similar to the results obtained in the laboratory. It is outstanding that we could see the interference fringes in different observables and not only in intensity as it is normally seen in academic courses.

5 Acknowledgment

We thank Tecnológico de Monterrey's professors Benjamin Perez-Garcia, Raul I. Hernandez-Aranda, Dorilián Lopez-Mago and Blas M. Rodriguez-Lara for their feedback, support and useful suggestions.

[1] Gossman, D., Perez-Garcia, B., Hernandez-Aranda, R., Forbes, A. (2016). Optical interference with digital holograms. American Journal of Physics, 508-516.

[2] Guenther, R. D. (1990). Modern Optics. United States: John Wiley and Sons.

[3] Hecht, E. (2017). Optics. United States: Pearson Education.

[4] E. Collett, Field Guide to Polarization, SPIE Press, Bellingham, WA (2005).

[5] Alexei D. Kiselev, e. a. (2018). Interferometric and Uhlmann phases of mixed polarization states. Research Gate, 3-5.

6 Appendix

6.1 Appendix A: Maths of Fringes in Intensity

Let's consider two monochromatic waves polarized in the same plane

$$E_1 = Ae^{-i\Phi_1}e^{i\omega t} \tag{13}$$

$$E_2 = Ae^{-i\Phi_2}e^{i\omega t} \tag{14}$$

We can sum them:

$$E = E_1 + E_2 \tag{15}$$

$$E = Ae^{i\omega t}[e^{-i\Phi_1} + e^{-i\Phi_2}] \tag{16}$$

We can compute the intensity:

$$\begin{aligned} I = |E^2| = \bar{E}E &= A^2[e^{-i\varphi_1} + e^{-i\varphi_2}][e^{i\varphi_1} + e^{i\varphi_2}] \\ &= A^2(e^{i\varphi_2 - i\varphi_1} + e^{-i\varphi_2 + i\varphi_1} + 2) \\ &= A^2\left(\frac{2(e^{i(\varphi_2-\varphi_1)} + e^{-i(\varphi_1-\varphi_2)})}{2} + 2\right) \\ &= A^2 2\left(\frac{2\cos(\varphi_1 - \varphi_2) + 1}{2}\right) \end{aligned}$$

$$I = 4A^2\cos^2\left(\frac{\varphi_1 - \varphi_2}{2}\right) \tag{17}$$

Where constructive interference is $\varphi_1 - \varphi_2 = 2\pi n$ and destructive is $\varphi_1 - \varphi_2 = (2n-1)\pi$, where $n \in \mathbb{Z}$ and $\varphi_1 = k_1 x$, $\varphi_2 = k_2 x$ We can rewrite the constructive interference in terms of x:

$$\varphi_1 - \varphi_2 = 2\pi n = k_1 - k_2 x = x(k_1 - k_2)$$

$$x = \frac{2\pi n}{k_1 - k_2} \tag{18}$$

The equation of intensity does not suggests any coordinate system, so, for example, we can construct azimutal fringes by the equivalences: $\varphi_1 = l\theta$ and $\varphi_2 = -l\theta$, where θ is the azimutal angle and l is the topological charge.
For constructive interference we obtain:

$$\varphi_1 - \varphi_2 = 2\pi n = l\theta - (-l\theta) = 2l\theta \quad \Longrightarrow \quad \theta = \frac{\pi n}{l} \tag{19}$$

To find radial fringes we can take $\varphi_1 = k_\rho \rho$, $\varphi_2 = 0$, where $\rho^2 = x^2 + y^2$. So, constructive interference:

$$\varphi_1 - \varphi_2 = k_\rho \rho - 0 = 2\pi n \quad \Longrightarrow \quad \rho = \frac{2\pi n}{k_\rho} \tag{20}$$

We can create many pinholes (fringes) in all positions, for example, to create a ring. We can state this by a sum:

$$E = \sum_{n=0}^{N} E_n \tag{21}$$

$$E = \sum_{n=0}^{N} Ae^{i\varphi_n} \tag{22}$$

where $\varphi_n = \mathbf{k} \cdot \mathbf{r}$. The superposition of plane waves arranged in a of $\mathbf{k}$ and $\mathbf{r}$ can be written as

$$\mathbf{k} = k\sin\theta\cos\phi\hat{\mathbf{x}} + k\sin\theta\sin\phi\hat{\mathbf{y}} + k\cos\theta\hat{\mathbf{z}} \tag{23}$$

$$\mathbf{r} = \rho\cos\alpha\hat{\mathbf{x}} + \rho\sin\alpha\hat{\mathbf{y}} + z\hat{\mathbf{z}} \tag{24}$$

where $\mathbf{r} = \mathbf{r}(\rho, \alpha, z)$ in polar (cylindrical) coordinates and $\mathbf{k}$ is written in spherical coordinates, with fixed value θ and $\phi \in [0, 2\pi]$. We can use the dot product $\varphi_n = \mathbf{k} \cdot \mathbf{r}$ in eq. (10):

$$E = \sum_{n=0}^{N} A \exp\left[i(k \sin\theta \cos\phi_n \rho \cos\alpha + k \sin\theta \sin\phi_n \rho \sin\alpha + kz\cos\theta)\right] \tag{25}$$

working with the varying argument, i.e. $\varphi_n = \mathbf{k} \cdot \mathbf{r}$:

$$\begin{aligned} \varphi_n &= k \sin\theta \rho(\cos\phi_n \cos\alpha + \sin\phi_n \sin\alpha) + kz\cos\theta \\ &= k\rho \sin\theta \cos(\phi_n - \alpha) + kz\cos\theta \end{aligned}$$

Therefore,

$$E = A \sum_{n=0}^{N} \exp\left[i(k\rho \sin\theta \cos(\phi_n - \alpha) + kz\cos\theta)\right] \tag{26}$$

If we do $N \to \infty$:

$$E = \lim_{N\to\infty} A e^{ikz\cos\theta} \sum_{n=0}^{N} e^{i(k\rho \sin\theta \cos(\phi_n - \alpha))} \tag{27}$$

When we compute the limit, the sum transforms into an integral over φ_n, where $\varphi_n \in [0, 2\pi]$. So, rewriting eq. (15):

$$E = A e^{ikz\cos\theta} \int_0^{2\pi} e^{i(k\rho \sin\theta \cos(\phi_n - \alpha))} d\phi \tag{28}$$

We can do the integral in eq. (16) using the definition of *Bessel Function* of zero order:

$$J_0(u) = \frac{1}{2\pi} \int_0^{2\pi} e^{iu\cos v} dv$$

To complete, we multiply eq. (16) by 2π and divide over the same factor. Also, let $u = k\rho\sin\theta$ and $v = \phi - \alpha$, $d\phi = dv$. Then, eq. (16) is:

$$E = 2\pi A e^{ikz\cos\theta} \frac{1}{2\pi} \int_0^{2\pi} e^{iu\cos v} dv = 2\pi A e^{ikz\cos\theta} J_0(u)$$

A can absorb the 2π factor, therefore

$$E = A e^{ikz\cos\theta} J_0(k\rho\sin\theta) \tag{29}$$

and the intensity is:

$$\begin{aligned} |E|^2 = \bar{E}E &= A e^{ikz\cos\theta} J_0^2(k\rho\sin\theta) A e^{-ikz\cos\theta} \\ I &= A^2 J_0^2(k\rho\sin\theta) \end{aligned} \tag{30}$$

6.2 Appendix B: Codes of Digitally creating fringes

6.2.1 Digital apertures code

```
% -------------- Azimuthal Map of Polarization ---------------
close all
S = 400; %number of points
%Definition of the grating using a diagonal pattern
%This is the "Base grating"
M = zeros(S);
lim = 18;
aux = 0;
for i = 1:S
    for j = 1:S
            M(i,j) = aux;
        if aux > (lim/2)+1
            M(i,j) = M(i,j)-aux+(lim/2);
        end
```

```
        if aux < lim
            aux = aux+1;
        else
            aux = 0;
        end
    end
end

%Creating a grating with a dephase of pi with respect the first
M1 = zeros(S);
lim = 18;
aux = 9; %Here is determined the phase
for i = 1:S
    for j = 1:S
            M1(i,j) = aux;
        if aux > (lim/2)+1
            M1(i,j) = M1(i,j)-aux+(lim/2);
        end
        if aux < lim
            aux = aux+1;
        else
            aux = 0;
        end
    end
end

%Creating a grating with a dephase of pi with respect the first
M2 = zeros(S);
lim = 18;
aux = 5; %Here is determined the phase
for i = 1:S
    for j = 1:S
            M2(i,j) = aux;
        if aux > (lim/2)+1
            M2(i,j) = M2(i,j)-aux+(lim/2);
        end
        if aux < lim
            aux = aux+1;
        else
            aux = 0;
        end
    end
end

%Creating a grating with a dephase of 3*pi/2 with respect the first
M3 = zeros(S);
lim = 18;
aux = 15; %Here is determined the phase
for i = 1:S
    for j = 1:S
            M3(i,j) = aux;
        if aux > (lim/2)+1
            M3(i,j) = M3(i,j)-aux+(lim/2);
        end
        if aux < lim
            aux = aux+1;
        else
            aux = 0;
```

```
        end
    end
end

%Diagram of the desired angular
BASE = 10*ones(S);
for i = 1:S
    for j = 1:S
        if j<i+1 && S-j>i
            BASE(i,j) = 0;
        elseif j>i+1 && j>S-i
            BASE(i,j) = 0;
        else
            BASE(i,j) = 5;
        end
    end
end
BASE(1,1) = 10;
figure(1)
surf(BASE)
colormap('gray');
shading interp
colorbar
set(gca,'XColor', 'none','YColor','none')

% Take the respective "triangle" of different phase
% Creating the grating of different phases
% Blazed grating
M4 = zeros(S);
for i = 1:S
    for j = 1:S
        if j<i+1
            M4(i,j) = M(i,j);
        elseif j>i+1
            M4(i,j) = M1(i,j);
        end
        if j<i+1 && S-j>i
            M4(i,j) = M2(i,j);
        elseif j>i+1 && j>S-i
            M4(i,j) = M3(i,j);
        end
    end
end
figure(2)
surf(M4)
colormap('gray');
shading interp
colorbar
set(gca,'XColor', 'none','YColor','none')

%Definition of the ring
n=S;
D=3;
D1=1;
D2=0.95;
D3=1;
x0=linspace(-D/2,D/2,n);
[x,y]=meshgrid(x0);
```

```
rectx=1.*(abs(x/D1)<=sqrt(D1.^2-y.^2));
recty=1.*(abs(y/D1)<=sqrt(D1.^2-x.^2));
rectx1=1.*(abs(x/D2)<=sqrt(D2.^2-y.^2));
recty2=1.*(abs(y/D2)<=sqrt(D2.^2-x.^2));
g=rectx.*recty-rectx1.*recty2; %Ring n it's simple way

figure(3)
surface(x,y,g)
colormap('gray');
shading interp
set(gca,'XColor', 'none','YColor','none')

A = M.*g; %Ring with the blazed grating
figure(4)
surface(x,y,A)
colormap('gray');
shading interp
colorbar
set(gca,'XColor', 'none','YColor','none')

%Arrange two pinholes
lim = 26;
n=S;
i=sqrt(-1);
z=300;
D=30;
D1=1;
D2=1;
SD=10; %Separation of the pinholes
m=1^6;
w0=1*10^(-3);
x0=linspace(-D,D,n);
x1=linspace(-D,D+SD,n);
y1=linspace(-D,D,n);
[x,y]=meshgrid(x0);
[s,e]=meshgrid(x1,y1);
rectx=1.*(abs(x/D1)<=sqrt(D1.^2-y.^2));
recty=1.*(abs(y/D1)<=sqrt(D1.^2-x.^2));
rectx1=1.*(abs(s/D2)<=sqrt(D2.^2-e.^2));
recty2=1.*(abs(e/D2)<=sqrt(D2.^2-s.^2));
g=rectx.*recty+rectx1.*recty2;
dots = M.*g; %Definition of the blazed pinholes

figure(5)
surface(x,y,g); %The two pinholes
colormap('gray')
shading interp
set(gca,'XColor', 'none','YColor','none')

figure(6)
surface(x,y,dots);
colormap('gray')
shading interp
set(gca,'XColor', 'none','YColor','none')
```

6.2.2 Experimental fringes code

Interference in Young experiment:

```
n=2024;
i=sqrt(-1);
z=300;
D=100;
D1=1;
D2=1;
SD=15;
m=1^6;
for ii=1:SD
    w0=1*10^(-3);
    x0=linspace(-D,D,n);
    x1=linspace(-D,D+ii,n);
    y1=linspace(-D,D,n);
    [x,y]=meshgrid(x0);
    [s,e]=meshgrid(x1,y1);
    l=1;
    f=10;
    k=2*pi/l;
    rectx=1.*(abs(x/D1)<=sqrt(D1.^2-y.^2));
    recty=1.*(abs(y/D1)<=sqrt(D1.^2-x.^2));
    rectx1=1.*(abs(s/D2)<=sqrt(D2.^2-e.^2));
    recty2=1.*(abs(e/D2)<=sqrt(D2.^2-s.^2));
    g=rectx.*recty+rectx1.*recty2;
    U0=g;
    FT1=fftshift(fft2(U0));
    if ii==5
            figure(1)
            subplot(1,2,1)
            imagesc(x0,x0,abs(U0));
            subplot(1,2,2)
            imagesc(x0,x0,abs(FT1))
            colormap('gray')
        elseif ii==10
            figure(2)
            subplot(1,2,1)
            imagesc(x0,x0,abs(U0));
            subplot(1,2,2)
            imagesc(x0,x0,abs(FT1))
            colormap('gray')
        elseif ii==15
            figure(3)
            subplot(1,2,1)
            imagesc(x0,x0,abs(U0));
            subplot(1,2,2)
            imagesc(x0,x0,abs(FT1))
            colormap('gray')
    end
end
```

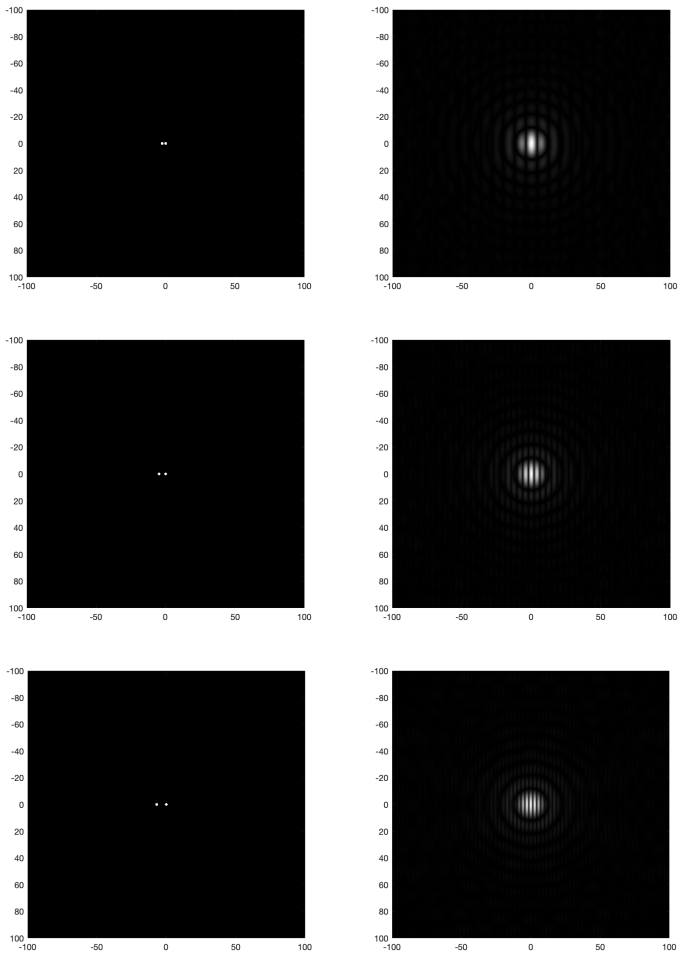

Figure 12: Young experiment with variation in the distance between the apertures.

Superposition of OAM modes with |l|=1,3,5:

```
close all
N=1024;
m=0;
n=5;
l=633e-9;
L = 1e-3;
dx = 2*L/N;
w0=1e-3;
x0=linspace(-4*w0,4*w0,N);
[x,y]=meshgrid(x0);
q0=(pi*w0.^2)/l;
Phi = atan2(y,x);
k=(2*pi)/l;
zr=k.*w0.^2/2;
z=1.5.*zr;
phi = atan(z/q0);
r=sqrt(x.^2+y.^2)/w0^2;
r1=(x.^2+y.^2);
for ii=0:n
    ft=((sqrt(2).*r)./(w0^2.*(1+(z./(q0)).^2))).^m;
    st=laguerreL(m,-ii);
    tt=((sqrt(2).*r)./(w0^2.*(1+(z./(q0)).^2))).^2;
    phase=exp(1i.*-ii.*Phi);
```

```
    nt=exp(-1i.*(2.*m-ii).*phi);
    gau=exp(-r1/w0^2);
    fmn1=ft.*st.*tt.*phase.*nt.*gau;
    ft1=((sqrt(2).*r)./(w0^2.*(1+(z./(q0)).^2))).^m;
    st1=laguerreL(m,ii);
    tt1=((sqrt(2).*r)./(w0^2.*(1+(z./(q0)).^2))).^2;
    phase1=exp(1i.*ii.*Phi);
    nt1=exp(1i.*(2.*m+ii).*phi);
    fmn2=ft1.*st1.*tt1.*phase1.*nt1.*gau;
    fmn=fmn1+fmn2;
    I1=abs(fmn1);
    I2=abs(fmn2);
    I3=abs(fmn);
    I4=angle(fmn1);
    I5=angle(fmn2);
    I6=angle(fmn);
    if ii==1
        figure(1)
        subplot(2,3,1)
        imagesc(x0,x0,I1);
        subplot(2,3,2)
        imagesc(x0,x0,I2);
        subplot(2,3,3)
        imagesc(x0,x0,I3)
        subplot(2,3,4)
        imagesc(x0,x0,I4);
        subplot(2,3,5)
        imagesc(x0,x0,I5);
        subplot(2,3,6)
        imagesc(x0,x0,I6);
        colormap('gray')
    elseif ii==3
        figure(2)
        subplot(2,3,1)
        imagesc(x0,x0,I1);
        subplot(2,3,2)
        imagesc(x0,x0,I2);
        subplot(2,3,3)
        imagesc(x0,x0,I3)
        subplot(2,3,4)
        imagesc(x0,x0,I4);
        subplot(2,3,5)
        imagesc(x0,x0,I5);
        subplot(2,3,6)
        imagesc(x0,x0,I6);
        colormap('gray')
    elseif ii==5
        figure(3)
        subplot(2,3,1)
        imagesc(x0,x0,I1);
        subplot(2,3,2)
        imagesc(x0,x0,I2);
        subplot(2,3,3)
        imagesc(x0,x0,I3)
        subplot(2,3,4)
        imagesc(x0,x0,I4);
        subplot(2,3,5)
        imagesc(x0,x0,I5);
```

```
82          subplot(2,3,6)
83          imagesc(x0,x0,I6);
84          colormap('gray')
85      end
86  end
```

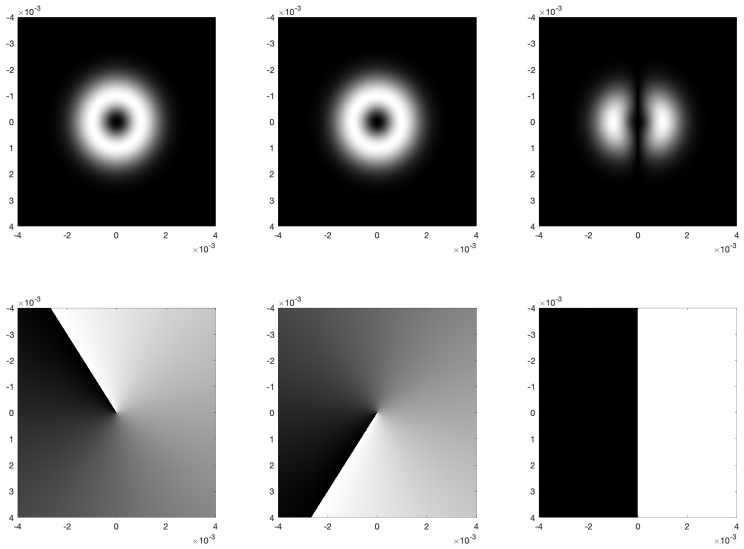

Figure 13: Superposition of OAM l=1

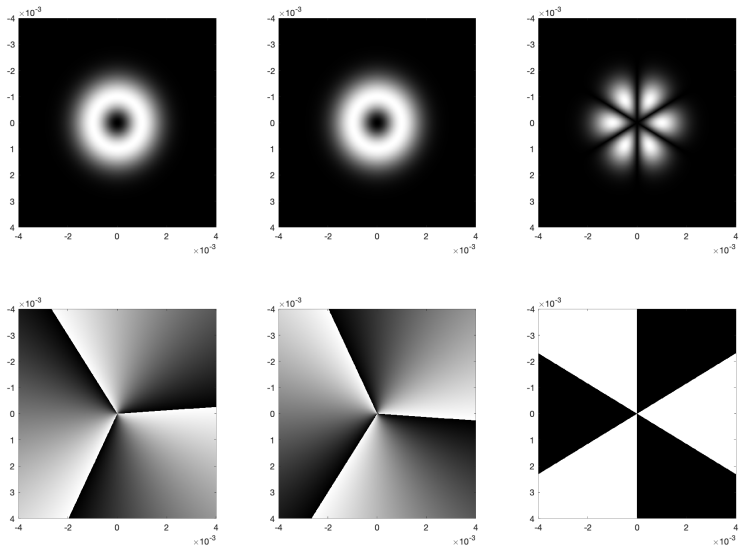

Figure 14: Superposition of OAM l=3

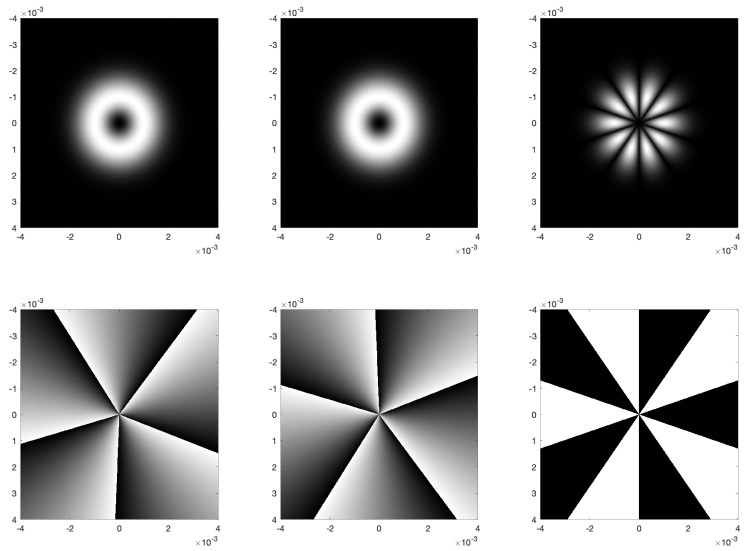

Figure 15: Superposition of OAM l=5

Interference pattern for small circular apertures

```
close all
noDots = 31;
i=sqrt(-1);
for jj = 1:noDots-1
    if jj==10
        clear all
        n=2048;
        U0=zeros(n);
        for rr = 1:10
            z=300;
            D=100;
            D1=0.45;
            D2=D1;
            m=1^6;
            w0=1*10^(-3);
            l = 1;
            k = 2*pi/l;
            x1 = linspace(-5,5,n);
            y1 = linspace(-5,5,n);
            [u,s] = meshgrid(x1,y1);
             [v,a] = pol2cart(linspace(0, 2*pi, 11), 11);
             x0=linspace(-D,D+v(rr),n);
             y0=linspace(-D,D+a(rr),n);
             [x,y]=meshgrid(x0,y0);
             circx=2.*(abs(x/D1)<=sqrt(D1.^2-(y).^2));
             circy=2.*(abs(y/D1)<=sqrt(D1.^2-(x).^2));
             g=circx.*circy;
             U0=U0+g;
             FT1=fftshift(fft2(U0));
             figure(1)
             subplot(1,2,1)
             imagesc(x1,y1,abs(U0))
             subplot(1,2,2)
             imagesc(x1,y1,abs(FT1))
             colormap('gray')
```

```
        end
    elseif jj==20
        clear all
        n=2048;
        U0=zeros(n);
        for ff = 1:20
            z=300;
            D=300;
            D1=1;
            D2=D1;
            m=1^6;
            w0=1*10^(-3);
            l = 1;
            k = 2*pi/l;
            x1 = linspace(-5,5,n);
            y1 = linspace(-5,5,n);
            [u,s] = meshgrid(x1,y1);
             [v,a] = pol2cart(linspace(0, 2*pi, 21), 21);
             x0=linspace(-D,D+v(ff),n);
             y0=linspace(-D,D+a(ff),n);
             [x,y]=meshgrid(x0,y0);
             circx=2.*(abs(x/D1)<=sqrt(D1.^2-(y).^2));
             circy=2.*(abs(y/D1)<=sqrt(D1.^2-(x).^2));
             g=circx.*circy;
             U0=U0+g;
             FT1=fftshift(fft2(U0));

             figure(2)
             subplot(1,2,1)
             imagesc(x1,y1,abs(U0))
             subplot(1,2,2)
             imagesc(x1,y1,abs(FT1))
             colormap('gray')
        end
    elseif jj==21
        clear all
        n=2048;
        U0=zeros(n);
        for ii = 1:20
            z=300;
            D=100;
            D1=0.45;
            D2=D1;
            m=1^6;
            w0=1*10^(-3);
            l = 1;
            k = 2*pi/l;
            x1 = linspace(-5,5,n);
            y1 = linspace(-5,5,n);
            [u,s] = meshgrid(x1,y1);
             [v,a] = pol2cart(linspace(0, 2*pi, 21), ii);
             x0=linspace(-D,D+v(ii),n);
             y0=linspace(-D,D+a(ii),n);
             [x,y]=meshgrid(x0,y0);
             circx=2.*(abs(x/D1)<=sqrt(D1.^2-(y).^2));
             circy=2.*(abs(y/D1)<=sqrt(D1.^2-(x).^2));
             g=circx.*circy;
             U0=U0+g;
```

```
                FT1=fftshift(fft2(U0));
                figure(3)
                subplot(1,2,1)
                imagesc(x1,y1,abs(U0))
                subplot(1,2,2)
                imagesc(x1,y1,abs(FT1))
                colormap('gray')
            end
        elseif jj==30
            clear all
            n=2048;
            U0=zeros(n);
            for ff = 1:30
                z=300;
                D=400;
                D1=5;
                D2=D1;
                m=1^6;
                w0=1*10^(-3);
                l = 1;
                k = 2*pi/l;
                x1 = linspace(-5,5,n);
                y1 = linspace(-5,5,n);
                [u,s] = meshgrid(x1,y1);
                 [v,a] = pol2cart(linspace(0, 2*pi, 31), 31);
                 x0=linspace(-D,D+v(ff),n);
                 y0=linspace(-D,D+a(ff),n);
                 [x,y]=meshgrid(x0,y0);
                 circx=2.*(abs(x/D1)<=sqrt(D1.^2-(y).^2));
                 circy=2.*(abs(y/D1)<=sqrt(D1.^2-(x).^2));
                 g=circx.*circy;
                 U0=U0+g;
                 FT1=fftshift(fft2(U0));
                 figure(4)
                 subplot(1,2,1)
                 imagesc(x1,y1,abs(U0))
                 subplot(1,2,2)
                 imagesc(x1,y1,abs(FT1))
                 colormap('gray')
                end
        end
end
```

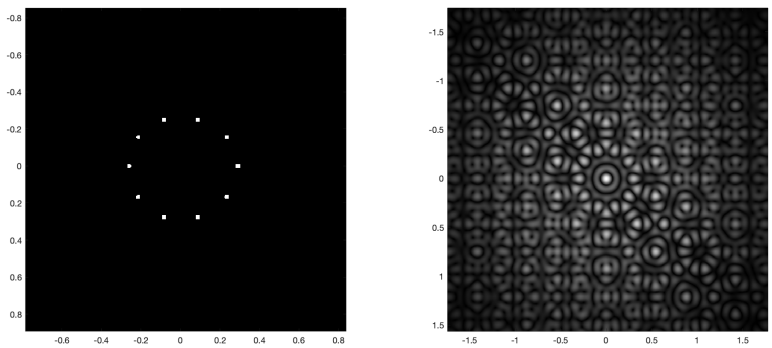

Figure 16: Circular arrange with 10 small apertures and interference pattern.

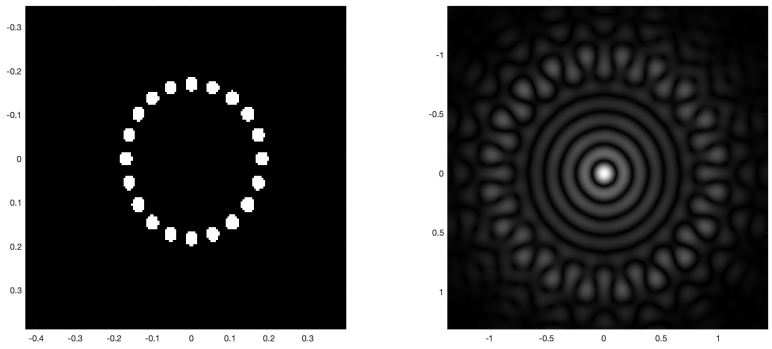

Figure 17: Circular arrange with 20 small apertures and interference pattern.

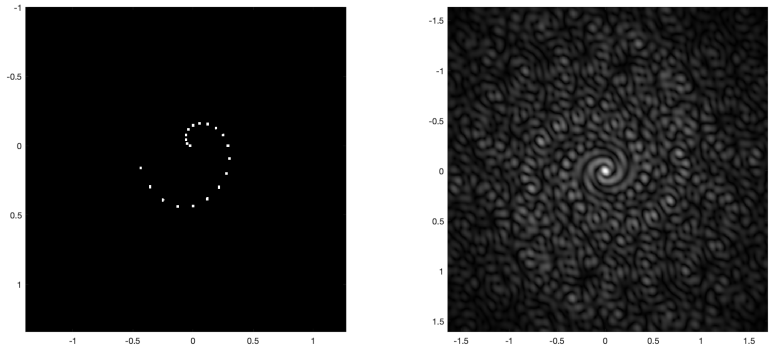

Figure 18: Spiral arrange with 20 small apertures and interference pattern.

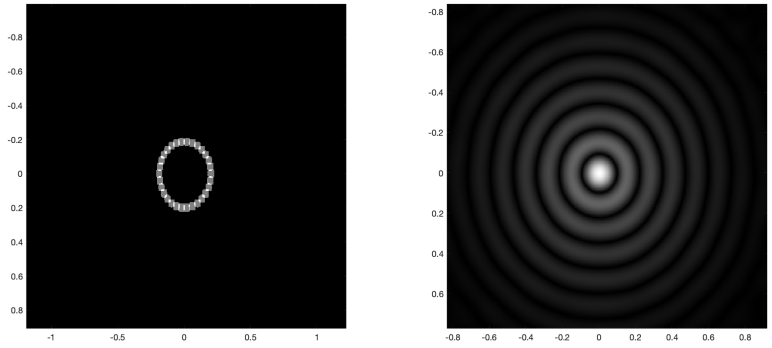

Figure 19: Ring and diffraction pattern.

6.3 Appendix C:Maths of fringes in polarization

We can express a vector field as:

$$\mathbf{E} = E_{0x}\cos(kz - \omega t + \varphi_1)\hat{x} + E_{0y}\cos(kz - \omega t + \varphi_2)\hat{y} \tag{31}$$

We can set φ_1 as reference and then use $\delta = \varphi_1 - \varphi_2$ Let us take the y-component

$$\mathbf{E}\cdot\hat{\mathbf{y}} = E_{0y}\cos(\mathbf{k}\cdot\mathbf{r} - \omega t + \delta) \tag{19.1}$$

$$\frac{E_y}{E_{0y}} = \cos(\mathbf{k}\cdot\mathbf{r} - \omega t + \delta) = \cos(\mathbf{k}\cdot\mathbf{r})\cos\delta - \sin(\mathbf{k}\cdot\mathbf{r})\sin\delta$$

We can calculate $\mathbf{E}\cdot\hat{\mathbf{x}}$ and multiply all by $\cos\delta$

$$\frac{E_x}{E_{0x}}\cos\delta = \cos\left(\mathbf{k}\cdot\mathbf{r}-\omega t\right)\cos\delta \tag{19.2}$$

Then, we can write:

$$\frac{E_y}{E_{0y}} - \frac{E_x}{E_{0x}} = -\sin\mathbf{k}\cdot\mathbf{r}-\omega t\sin\delta \tag{19.3}$$

Retake $\dfrac{E_x}{E_{0x}} = \cos\left(\mathbf{k}\cdot\mathbf{r}-\omega t\right)$ and square both sides

$$\left(\frac{E_x}{E_{0x}}\right)^2 = \cos^2\left(\mathbf{k}\cdot\mathbf{r}-\omega t\right) = 1-\sin^2\left(\mathbf{k}\cdot\mathbf{r}-\omega t\right) \tag{19.4}$$

We can square eq. (19.3) and use eq. (19.4) to obtain

$$\left[\frac{E_y}{E_{0y}} - \frac{E_x}{E_{0x}}\cos\delta\right]^2 = \left[1-\left(\frac{E_x}{E_{0x}}\right)^2\right]\sin^2\delta$$

Let us expand:

$$\left(\frac{E_y}{E_{0y}}\right)^2 + \left(\frac{E_x}{E_{0x}}\right)^2(1-\sin^2\delta) - 2\frac{E_x}{E_{0x}}\frac{E_y}{E_{0y}}\cos\delta = \left[1-\left(\frac{E_x}{E_{0x}}\right)^2\right]\sin^2\delta$$

Finally, we obtain the polarization ellipse equation:

$$\left(\frac{E_x}{E_{0x}}\right)^2 + \left(\frac{E_y}{E_{0y}}\right)^2 - 2\frac{E_x}{E_{0x}}\frac{E_y}{E_{0y}}\cos\delta = \sin^2\delta \tag{32}$$

The general polarization state is an ellipse which basis are:

$$\hat{\mathbf{e_1}} = \frac{1}{\sqrt{2}}e^{i\varphi_1}\hat{\mathbf{x}} + \frac{1}{\sqrt{2}}e^{i\varphi_2}\hat{\mathbf{y}} \tag{33}$$

$$\hat{\mathbf{e_2}} = \frac{1}{\sqrt{2}}e^{-i\varphi_2}\hat{\mathbf{x}} + \frac{1}{\sqrt{2}}e^{-i\varphi_1}\hat{\mathbf{y}} \tag{34}$$

To generate polarization fringes, we considered the following orthogonal supper position:

$$\mathbf{E}(x,y) = A_1(x,y)e^{i\varphi_1}\hat{\mathbf{x}} + A_2(x,y)e^{i\varphi_2}\hat{\mathbf{y}} \tag{35}$$

where$A_1 = A_2 = A$. Now, we can rewrite the supper position in terms of the elliptical basis:

$$\mathbf{E}(x,y) = \sqrt{2}A\left(\frac{(e^{i\varphi_1}\hat{\mathbf{x}} + e^{i\varphi_2}\hat{\mathbf{y}})}{\sqrt{2}}\right) = \sqrt{2}A(x,y)\hat{\mathbf{e_1}} \tag{36}$$

And the constructive interference condition of the diagonal components reads:

$$x = \frac{2\pi n}{k_1 - k_2} \tag{37}$$

For radial fringes in polarization, constructive interference:

$$\rho = \frac{2\pi n}{k_\rho} \tag{38}$$

And the azimutal constructive interference

$$\theta = \frac{\pi n}{l} \tag{39}$$

6.4 Appendix D: Codes of Fringes in Polarization

Diagonal and antidiagonal proyections for linear polarization

```
n=2024;
i=sqrt(-1);
z=300;
D=100;
D1=1;
D2=D1;
SD=10;
m=1^6;
N=2;
df=1;
q=N*pi/df;
w0=1*10^(-3);
x0=linspace(-D,D,n);
x1=linspace(-D,D+SD,n);
y1=linspace(-D,D,n);
[x,y]=meshgrid(x0);
[s,e]=meshgrid(x1,y1);
l=1;
f=10;
k=2*pi/l;
rectx=1.*(abs(x/D1)<=sqrt(D1.^2-y.^2));
recty=1.*(abs(y/D1)<=sqrt(D1.^2-x.^2));
rectx1=1.*(abs(s/D2)<=sqrt(D2.^2-e.^2));
recty2=1.*(abs(e/D2)<=sqrt(D2.^2-s.^2));
g=rectx.*recty+rectx1.*recty2.*4;
g2=rectx.*recty-4.*rectx1.*recty2;
FT1=fftshift(fft2(g));
FT2=fftshift(fft2(g2));
FT1a=abs(FT1);
FT2b=abs(FT2);
I=FT1a+FT2b;
figure(1)
subplot(2,2,1)
imagesc(x0,x0,abs(g));
subplot(2,2,2)
imagesc(x0,x0,FT1a);
subplot(2,2,3)
imagesc(x0,x0,FT2b);
subplot(2,2,4)
imagesc(x0,x0,I)
colormap('gray')
```

Diagonal and antidiagonal proyections for azimuthal polarization

```
close all
N=1024;
m=0;
n=2;
df=1;
l=633e-9;
L = 1e-3;
dx = 2*L/N;
w0=1e-3;
x0=linspace(-4*w0,4*w0,N);
[x,y]=meshgrid(x0);
q0=(pi*w0.^2)/l;
```

```
Phi = atan2(y,x);
k=(2*pi)/l;
zr=k.*w0.^2/2;
z=1.5.*zr;
z2=zr;
phi = atan(z/q0);
phi2 = atan(z2/q0);
r=sqrt(x.^2+y.^2)/w0^2;
r1=(x.^2+y.^2);
q=n*pi/df;
ft=20;
st=-besselj(m,r1./w0^(2.2));
nt=exp(-1i.*m.*q.*df);
gau=exp(-r1/w0^2);
fmn1=ft.*st.*nt.*gau+q;
ft1=20;
st1=besselj(m,r1./w0^(2.2));
nt1=exp(-1i.*m.*q.*df);
gau1=exp(-r1/w0^2);
fmn2=ft1.*st1.*nt1.*gau1+q;
I1=abs(fmn1);
I2=abs(fmn2);
I=I1+I2;
figure(1)
subplot(1,3,1)
imagesc(x0,x0,I1)
subplot(1,3,2)
imagesc(x0,x0,I2)
subplot(1,3,3)
imagesc(x0,x0,I)
colormap('gray')
```

Diagonal and antidiagonal proyections for radial polarization

```
close all
N=1024;
m=1;
n=-3;
s=3;
l=633e-9;
L = 1e-3;
dx = 2*L/N;
w0=1e-3;
x0=linspace(-4*w0,4*w0,N);
[x,y]=meshgrid(x0);
q0=(pi*w0.^2)/l;
Phi = atan2(y,x);
k=(2*pi)/l;
zr=k.*w0.^2/2;
z=1.5.*zr;
phi = atan(z/q0);
r=sqrt(x.^2+y.^2)/w0^2;
r1=(x.^2+y.^2);
ft=((sqrt(2).*r)./(w0^2.*(1+(z./(q0)).^2))).^m;
st=laguerreL(m,n);
tt=((sqrt(2).*r)./(w0^2.*(1+(z./(q0)).^2))).^2;
phase=exp(1i.*n.*Phi);
nt=exp(1i.*(2.*m+n).*phi);
gau=exp(-r1/w0^2);
```

```
fmn1=ft.*st.*tt.*phase.*nt.*gau;
ft1=((sqrt(2).*r)./(w0^2.*(1+(z./(q0)).^2))).^m;
st1=laguerreL(m,s);
tt1=((sqrt(2).*r)./(w0^2.*(1+(z./(q0)).^2))).^2;
phase1=exp(1i.*s.*Phi);
nt1=exp(1i.*(2.*m+s).*phi);
fmn2=ft1.*st1.*tt1.*phase1.*nt1.*gau;
fmn=fmn1+fmn2;
ft2=((sqrt(2).*r)./(w0^2.*(1+(z./(q0)).^2))).^m;
st2=-laguerreL(m,n);
tt2=((sqrt(2).*r)./(w0^2.*(1+(z./(q0)).^2))).^2;
phase2=exp(1i.*n.*Phi);
nt2=exp(1i.*(2.*m+n).*phi);
fmn3=ft2.*st2.*tt2.*phase2.*nt2.*gau;
ft3=((sqrt(2).*r)./(w0^2.*(1+(z./(q0)).^2))).^m;
st3=laguerreL(m,s);
tt3=((sqrt(2).*r)./(w0^2.*(1+(z./(q0)).^2))).^2;
phase3=exp(1i.*s.*Phi);
nt3=exp(1i.*(2.*m+s).*phi);
fmn4=ft3.*st3.*tt3.*phase3.*nt3.*gau;
fmnsec=fmn3+fmn4;
I=abs(fmn+fmnsec);
figure(1)
subplot(1,3,1)
imagesc(x0,x0,abs(fmn))
subplot(1,3,2)
imagesc(x0,x0,abs(fmnsec))
subplot(1,3,3)
imagesc(x0,x0,I)
colormap('gray')
```

Map of Linear Polarization

```
% -------------- Linear Map of Polarization ---------------
close all
n = 37;
D = 2*pi;
E0x = 20; %Amplitud x component
E0y = 20; %Amplitud y component
i = sqrt(-1);
Space = linspace(-D,D,n);
%Space2= linspace(-pi/2,pi/2,n);
ex = E0x*(cos(Space)+i*sin(Space)); %coordinate X
ey = E0y*(cos(Space)+i*sin(Space)); %coordinate Y
[Ex,Ey] = meshgrid(ex,ey);

% Stokes Vectors:
S0 = abs(Ex).^2+abs(Ey).^2;
S1 = abs(Ex).^2-abs(Ey).^2;
S2 = 2.*real(Ex.*conj(Ey));
S3 = 2.*imag(Ex.*conj(Ey));
%Parameters for elipses
Ip = sqrt(S1.^2+S2.^2+S3.^2);
L = S1+i*S2;

%Semiaxis, helicity and angles of each elipse
A = sqrt((Ip+abs(L))/2).*exp(-0.05*Space.^2);
B = sqrt((Ip-abs(L))/2).*exp(-0.05*Space.^2);
phi = (angle(L))/2;
```

```
H = sign(S3);
factor = 0.1;

%Parametric plot of each elipse
%Once we have their parameters
for ii = 1:n
    for jj = 1:n
        theta = phi(ii,jj);
        r1 = factor*A(ii,jj);
        r2 = factor*B(ii,jj);
        % calculo de los puntos del elipse
        t = linspace(0, 2.*pi, 100);
        xt = (r1 * cos(t));
        yt = (r2 * sin(t));
        % compute the points of each elipse
        cot = cos(theta)-sin(theta);
        sit = sin(theta)+cos(theta);
        xp = xt * cot - yt * sit-(jj-1)*10;
        yp = (xt * sit + yt * cot+(ii-1)*10);

        hold on

        plot(real(xp), real(yp), 'r');
    end
end
```

Map of Radial Polarization

```
% -------------- Radial Map of Polarization ---------------
close all
n = 57;  %No. elpises per side
i = sqrt(-1);
D1 = 1;
D = linspace(0.8,1.2,10);%Definition of radius of the rings
U0x = ones(n);
U0y = ones(n);
for ii = 1:length(D)
    %Creation of X  & Y components of the fields
    %Sinusoidal radial variation
    x0=linspace(-D1,D1,n);
    y0=linspace(-D1,D1,n);
    [x,y]=meshgrid(x0,y0);
    circx=(cos((ii-1)*pi/7)+i*sin((ii)*pi/2))*(abs(x/D(ii))>=sqrt(D(ii).^2-(y).^2));
    circy=(cos((ii-1)*pi/7)+i*sin((ii)*pi/2))*(abs(y/D(ii))>=sqrt(D(ii).^2-(x).^2));
    g=circx.*circy;
    U0x=U0x+circx;
    U0y=U0y+circy;
end
Ex = U0x;
Ey = U0y;
% Stokes Vectors:
S0 = abs(Ex).^2+abs(Ey).^2;
S1 = abs(Ex).^2-abs(Ey).^2;
S2 = 2.*real(Ex.*conj(Ey));
S3 = 2.*imag(Ex.*conj(Ey));
%Parameters for elipses
Ip = sqrt(S1.^2+S2.^2+S3.^2);
L = S1+i*S2;
%Semiaxis, helicity and angles of each elipse
```

```
phi = (atan(S2./S1));
A = sqrt((Ip+abs(L))/2);
B = sqrt((Ip-abs(L))/2);
H = sign(S3);

%Parametric plot of each elipse
%Once we have their parameters
for ii = 1:n

    for jj = 1:n
        theta = phi(ii,jj)+pi/4;
        r1 = A(ii,jj);
        r2 = 3*B(ii,jj);
        % compute the points of each elipse
        t = linspace(0, 2*pi, 20);
        xt = (r1 * cos(t));
        yt = (r2 * sin(t));

        cot = cos(theta);
        sit = sin(theta);
        xp = xt * cot - yt * sit-(jj-1)*10 ;
        yp = xt * sit + yt * cot+(ii-1)*10;

        hold on
        plot(real(xp), real(yp), 'k');
    end
end
```

Map of Azimuthal Polarization

```
% -------------- Azimuthal Map of Polarization ---------------
close all
n = 37; %No. elpises per side
i = sqrt(-1);
D1 = 1;
D = linspace(0.4,1,12);
U0x = zeros(n);
U0y = zeros(n);
x0=linspace(-D1,D1,n);
y0=linspace(-D1,D1,n);
[x,y]=meshgrid(x0,y0);
for ii = 1:length(D)
    %Creation of X  & Y components of the fields
    circx=0.8*(atan((ii-1))+i*sin((ii)*pi/2))*(abs(x/D(ii))>=sqrt(D(ii).^2-(y).^2));
    circy=0.8*(atan((ii-1))+i*sin((ii)*pi/2))*(abs(y/D(ii))>=sqrt(D(ii).^2-(x).^2));
    g=circx.*circy;
    U0x=U0x+circx;
    U0y=U0y+circy;
end
%Decay factor
decaimiento = 1*(abs(x/D(end))<=sqrt(D(end).^2-(y).^2));
Ex = U0x.*decaimiento; %X component
Ey = U0y.*decaimiento; %Y component
% Stokes Vectors:
S0 = abs(Ex).^2+abs(Ey).^2;
S1 = abs(Ex).^2-abs(Ey).^2;
S2 = 2.*real(Ex.*conj(Ey));
S3 = 2.*imag(Ex.*conj(Ey));
%Parameters for elipses
```

```
Ip = sqrt(S1.^2+S2.^2+S3.^2);
L = S1+i*S2;
%Semiaxis, helicity and angles of each elipse
A = sqrt((Ip+abs(L))/2);
B = sqrt((Ip-abs(L))/2);
phi = (angle(L))/2;
H = sign(S3);

%Parametric plot of each elipse
%Once we have their parameters
for ii = 1:n

    for jj = 1:n
        if ii == (n+1)/2 || jj == (n+1)/2
            B(ii,jj)  = 0;
            B(ii+1,jj+1)  = 0;
            B(ii+2,jj+2)  = 0;
        end
        theta = phi(ii,jj);
        r1 = 0.5*A(ii,jj);
        r2 = 1.5*B(ii,jj);
        % compute the points of each elipse
        t = linspace(0, 2*pi, 20);
        xt = (r1 * cos(t));
        yt = (r2 * sin(t));

        cot = cos(theta);
        sit = sin(theta);
        xp = xt * cot - yt * sit-(jj-1)*9;
        yp = xt * sit + yt * cot+(ii-1)*9;

        hold on

        plot(real(xp), real(yp), 'k');
        set(gca,'XColor', 'none','YColor','none')
    end
end
```

6.5 Appendix E: Maths of Fringes in Orbital Angular Momentum

The Fourier transforms are a pair of equations that can be described as:

$$\tilde{\psi}(\mathbf{k}) = \frac{1}{\sqrt{2\pi}} \int \psi(\mathbf{r}) \exp(-i\mathbf{k}\cdot\mathbf{r}) d\mathbf{r} \tag{40}$$

and

$$\psi(\mathbf{r}) = \frac{1}{\sqrt{2\pi}} \int \tilde{\psi}(\mathbf{k}) \exp(i\mathbf{k}\cdot\mathbf{r}) d\mathbf{k} \tag{41}$$

where ψ is the field, $\mathbf{r}$ is the linear position, and $\mathbf{k}$ is linear momentum in a three-dimensional space. Recreating Young's experiment, where the two slits on the screen can be considered as points, the field can be written as the following expression

$$\phi(\mathbf{r}) = \delta(\mathbf{r} - \mathbf{r_0}) + \delta(\mathbf{r} + \mathbf{r_0}) \tag{42}$$

where $\mathbf{r_0}$ is the position of the slit with respect to the origin. Now, we can translate these equations to an angular momentum frame, replacing the linear variables with its angular equivalents, and applying the same Fourier transformations:

$$\tilde{\psi}_l = \frac{1}{\sqrt{2\pi}} \int \psi(\theta) \exp(-il\theta) d\theta \tag{43}$$

and

$$\psi(\theta) = \frac{1}{\sqrt{2\pi}} \sum_{-\infty}^{\infty} \tilde{\psi}_l \exp(il\theta) \tag{44}$$

In this case, the slits are no longer individual points but rather cake-like slices, as mentioned on the main text. This means that we cannot represent the field equation as a sum of delta functions, but rather express it in the following way:

$$\psi(\theta) = rect\left(\frac{\theta - \theta_0}{\epsilon}\right) + rect\left(\frac{\theta - (\theta_0 + \pi)}{\epsilon}\right) \tag{45}$$

where θ_0 is the angular location of the slit, ϵ is its angular size, and $rect$ is the rectangular function.

We therefore use its correspondent Fourier transform to develop an expression for its angular momentum representation:

$$\tilde{\psi}_l = \frac{\epsilon}{\sqrt{2\pi}} sinc(\epsilon l/2) \left[e^{-il\theta_0} + e^{-il(\theta_0+\pi)}\right] \tag{46}$$

We can see, as stated in Section 2.4, that due to the rectangular nature of $\psi(\theta)$, its Fourier transform has a cardinal sine-type of envelope. Furthermore, the arguments for the two rectangular functions in the initially proposed equation are now expressed through a complex exponential, in terms of the spiral harmonics $\exp(-il\theta_0)$. So while the diffraction pattern of a single slit is the continuous intensity variation of linear momentum, or position in the far field, angular diffraction results in a square cardinal sine envelope of discrete OAM modes. We will see this once we compute the spectral distribution of the fringes in OAM:

$$I_l = |\tilde{\psi}_l|^2 = \frac{2\epsilon^2}{\pi} sinc^2(\epsilon l/2) \cos^2(\pi l/2) \tag{47}$$

Thanks to Euler's identity, we can express the exponentials in terms of sines and cosines, and due to the discretion of the variable l and the π term, the exponentials, when squared, give as a result a value of $4\cos^2(\pi l/2)$.

6.6 Appendix F: Codes of Fringes in Orbital Angular Momentum

Azimutal apertures and interference

```
%Creation of the interference pattern
n=2048;
D=10;
D1=1;
grados = 10;
x0=linspace(-D,D,n);
y0=linspace(-D,D,n);
[x,y]=meshgrid(x0,y0);
%Azimutal apertures
trigy1=2.*(abs(y/D1))<=tan(abs(0.5*x)); %Angular apertures
limCirc=1.*(abs(y/D1)<=sqrt(0.6*D1.^2-(x).^2)); %Delimiting polar circle
U0=trigy1.*limCirc;
FT1=fftshift(fft2(U0)); %Creation of the interference pattern

figure(1)
subplot(1,2,1)
imagesc(x0,x0,abs(U0))
set(gca,'XColor', 'none','YColor','none')
subplot(1,2,2)
imagesc(x0,x0,(abs(FT1)).^2);
colormap ('gray');
set(gca,'XColor', 'none','YColor','none')
```